

Supporting Information

A Cu₂Se-Cu₂O Film Electrodeposited on Titanium Foil as a Highly Active and Stable Electrocatalyst for the Oxygen Evolution Reaction

Hu Chen^a, Yan Gao^{*a}, Lu Ye^a, Yanan Yao^a, Xuyang Chen^a, Yu Wei^a, and Licheng Sun^{a,b}

^aState Key Laboratory of Fine Chemicals, Institute of Artificial Photosynthesis, DUT-KTH Joint Education and Research Center on Molecular Devices, Dalian University of Technology (DUT), Dalian 116024, China

^bDepartment of Chemistry, School of Chemical Science and Engineering, KTH Royal Institute of Technology, 10044 Stockholm, Sweden

* Corresponding author

E-mail addresses: dr.gaoyan@dlut.edu.cn (Y. Gao)

Experimental Section

1. General chemicals and materials

All chemicals, including copper sulfate pentahydrate ($\text{CuSO}_4 \cdot 5\text{H}_2\text{O}$), selenium dioxide (SeO_2), sodium bicarbonate (NaHCO_3), sodium hydroxide (NaOH), hydrochloric acid (HCl , ~37%) and Titanium foil (TF, thickness: 0.1 mm, purity: $\text{Ti} \geq 99.99\%$) were purchased from commercial suppliers and used without further purification. Milli-Q ultrapure water of $18.2 \text{ M}\Omega \cdot \text{cm}$ was applied in all experiments.

2. Preparation of the $\text{Cu}_2\text{Se-Cu}_2\text{O/TF}$, Cu/TF , CuO/TF electrodes and the carbonate buffer solution

Firstly, TF substrates were sonicated in a 2.0 M HCl for 30 min to remove the surface oxides and pollutants, and rinsed subsequently with water and ethanol. The clean and bare TF substrates were obtained for next use after drying under $100 \text{ }^\circ\text{C}$ over 2 h. The $\text{Cu}_2\text{Se-Cu}_2\text{O/TF}$ electrodes were prepared according to the following steps. The anodes were formed by the electrodeposition method, which was carried out in an aqueous solution (50 mM $\text{CuSO}_4 \cdot 5\text{H}_2\text{O}$ and 25 mM SeO_2) from a conventional three-electrode configuration with a TF substrate as the working electrode, saturated Ag/AgCl as the reference electrode, and Pt mesh as the auxiliary electrode. Electrodeposition was conducted by controlled potential electrolysis at -0.65 V (vs. Ag/AgCl) for 600 s at room temperature. After deposition, the $\text{Cu}_2\text{Se-Cu}_2\text{O/TF}$ electrode was rinsed with deionized water thoroughly. The Cu/TF electrodes were prepared by the similarly electrodeposited method without using Se precursor (SeO_2). The CuO/TF electrodes were obtained via calcination of the Cu/TF electrodes at $350 \text{ }^\circ\text{C}$ for 3 h in the air. The carbonate buffer solution (0.2 M, pH 11.0) as electrolyte for electrochemical measurements was prepared by dissolving NaHCO_3 (0.2 M) in ultrapure water and the pH value of the solution was adjusted to 11.0 by NaOH (solid).

3. The characterization of the electrodes

The scanning electron microscopy (SEM) images, the energy-dispersive X-ray (EDX) spectrum analysis and elemental distributions mapping were taken with a FEI Nova Nano SEM 450 instrument (3 kV) equipped with the energy-dispersion X-ray fluorescence analyzer. Transmission electron

microscopy (TEM) images and higher-resolution transmission electron microscopy (HRTEM) images were obtained with FEI TF30 equipment. The X-ray diffraction (XRD) patterns of the electrodes were recorded by D/max-2400 diffractometer with Cu-K α radiation source. The measurement was performed from 10° to 80° with a scan-rate of 8 °/min. X-ray photoelectron spectroscopy (XPS) measurements were performed on a Thermo VG ESCALAB 250X using Al K α radiation as the excitation source. The binding energy was calibrated according to C 1s neutral carbon peak at 284.8 eV.

4. Electrochemical measurements

All electrochemical experiments were carried out using a CHI Instruments Electrochemical Analyzer (CHI 660E) at room temperature (25 \pm 2 °C). The water oxidation performance of the Cu₂Se-Cu₂O/TF electrode was estimated from linear scan voltammetry (LSV) plots while the stability of the catalyst was studied by chronopotentiometry method. The electrochemical measurements were performed in a three-electrode system: the Cu₂Se-Cu₂O/TF electrode, the Ag/AgCl electrode and Pt mesh as work electrode, reference electrode and counter electrode, respectively. The reference electrode was calibrated by Ru(bpy)₃ (1.26 V vs. NHE) before using. The 100% iR-corrected was applied in the LSV and chronopotentiometry experiments. All the potentials were displayed versus reversible hydrogen electrode (RHE) by: $E(\text{RHE}) = E(\text{Ag/AgCl}) + 0.191 + 0.059 \times \text{pH}$. All of the current density in this paper was calculated based on the geometric area of electrode. The LSV measurements were executed under the scan rate of 5 mV/s. Moreover, the chronopotentiometry experiment was performed at a constant current density of 10 mA/cm² under gently stirring. At last, the Faradaic efficiency of the Cu₂Se-Cu₂O/TF electrode was carried out in a single gas-tight cell (total volume of 126 mL) equipped with Cu₂Se-Cu₂O/TF electrode (1.0 cm² active area) as the working electrode, Ag/AgCl as the reference electrode and Pt mesh as the counter electrode. The carbonate buffer electrolyte of 50.0 mL was added in electrolytic cell. Then, the electrolyte solution was degassed by bubbling Ar for 1 h to remove the air. Then the electrolysis was carried out at a stable current density of 10 mA/cm² without iR compensation in static electrolyte solution (0.2 M, pH = 11.0) for 2 h. The amount of evolved oxygen in the headspace was measured by gas chromatograph (GC 7890T instrument equipped with a thermal conductive detector) during electrolysis. The Faradic efficiency was calculated as $\text{O}_2(\text{actual})/\text{O}_2(\text{theoretical}) \times 100\%$. The ECSA was determined by measuring the

capacitive current associated with double-layer charging from the scan-rate dependence of CVs. For this, the potential window of CVs was 1.39–1.49 V vs. RHE. The scan rates were 2, 4, 6, 8 and 10 mV/s. The double-layer capacitance (C_{dl}) was estimated by plotting the $\Delta J = (J_a - J_c)$ at 1.44 V vs. RHE against the scan rate. The linear slope is twice of the double-layer capacitance C_{dl} . Electrochemical impedance spectrum (EIS) was recorded at 1.84 V vs. RHE over a frequency range from 10^6 to 0.1 Hz. In order to obtain the values of charge transfer resistances during OER, the Randles equivalent circuit method was used to fit experimental data. Here, **R1** is the resistance of the electrolyte; **CPE1** and **Rct** are the double-layer capacitance and charge transfer resistance, respectively, of the electrode in the electrolyte.

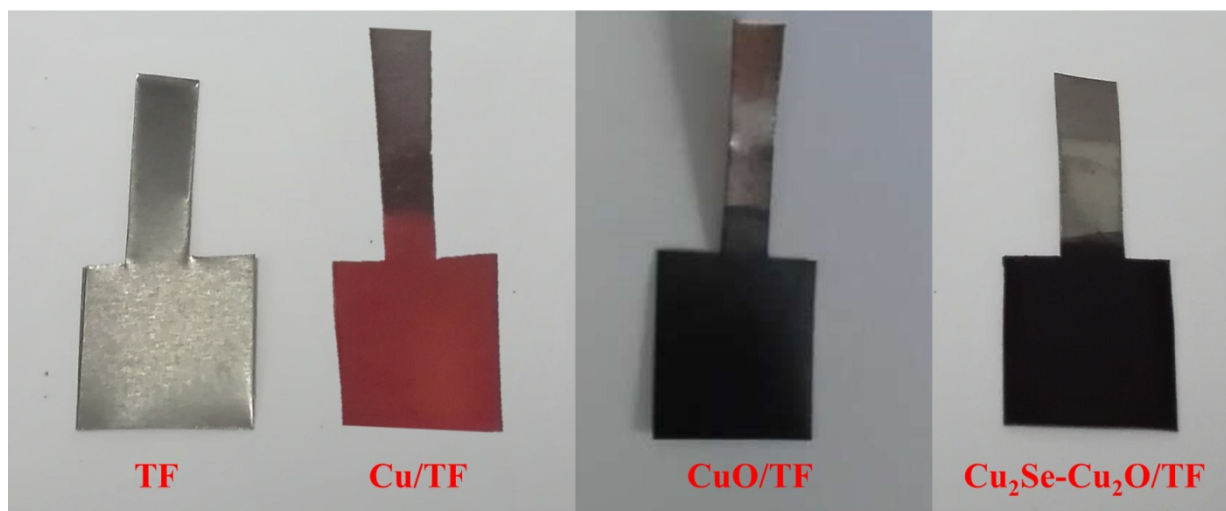


Figure S1. Photographs of the TF, Cu/TF, CuO/TF and Cu₂Se-Cu₂O/TF electrodes.

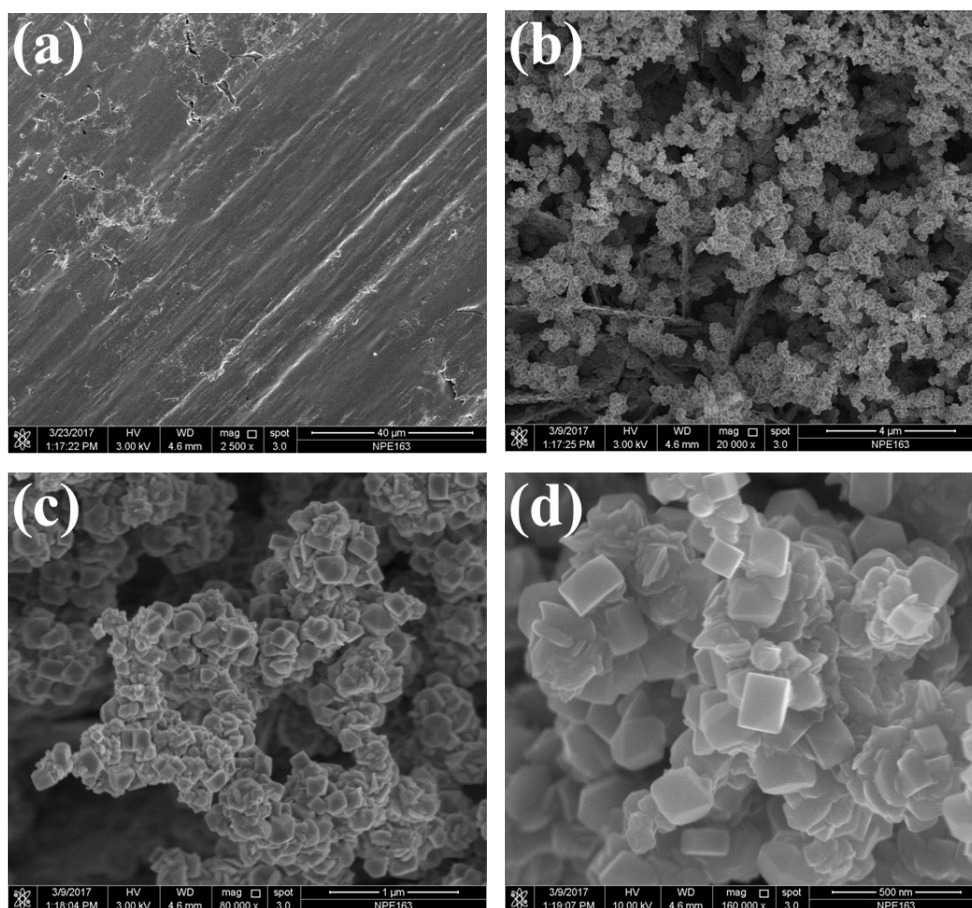


Figure S2. The SEM images of the bare TF (a) and $\text{Cu}_2\text{Se-Cu}_2\text{O/TF}$ (b, c, d).

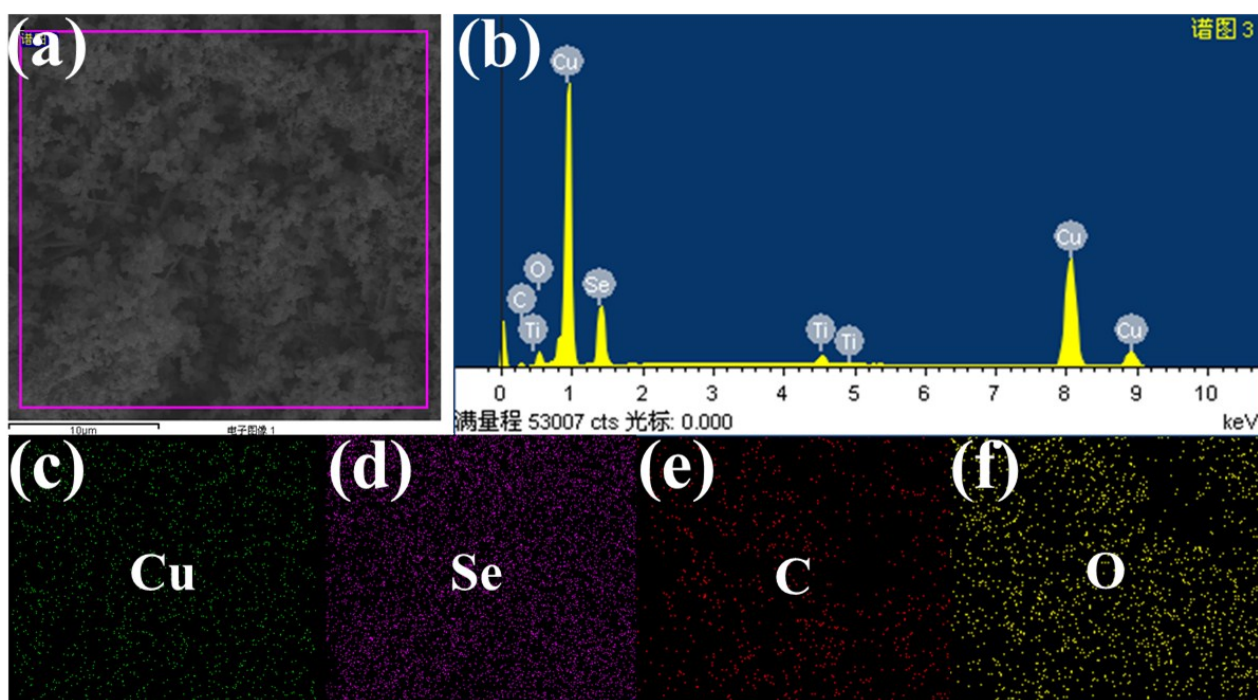


Figure S3. The SEM image (a) and EDX spectrum (b) of the $\text{Cu}_2\text{Se-Cu}_2\text{O/TF}$ electrode. Elemental mapping images (c, d, e, f) of the corresponding elements in the $\text{Cu}_2\text{Se-Cu}_2\text{O/TF}$ electrode.

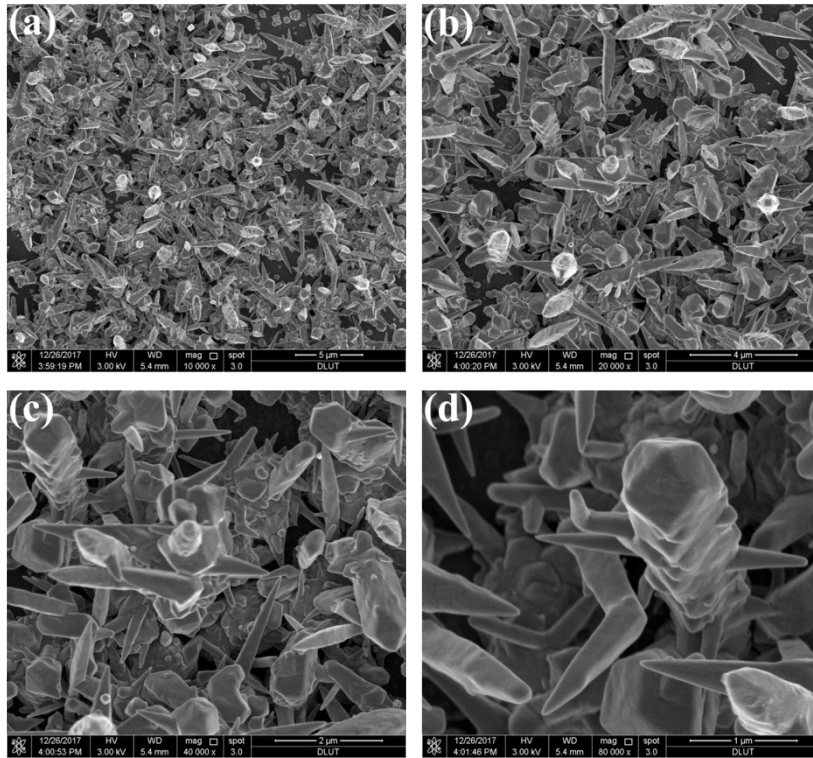


Figure S4. The SEM images of the Cu/TF electrode.

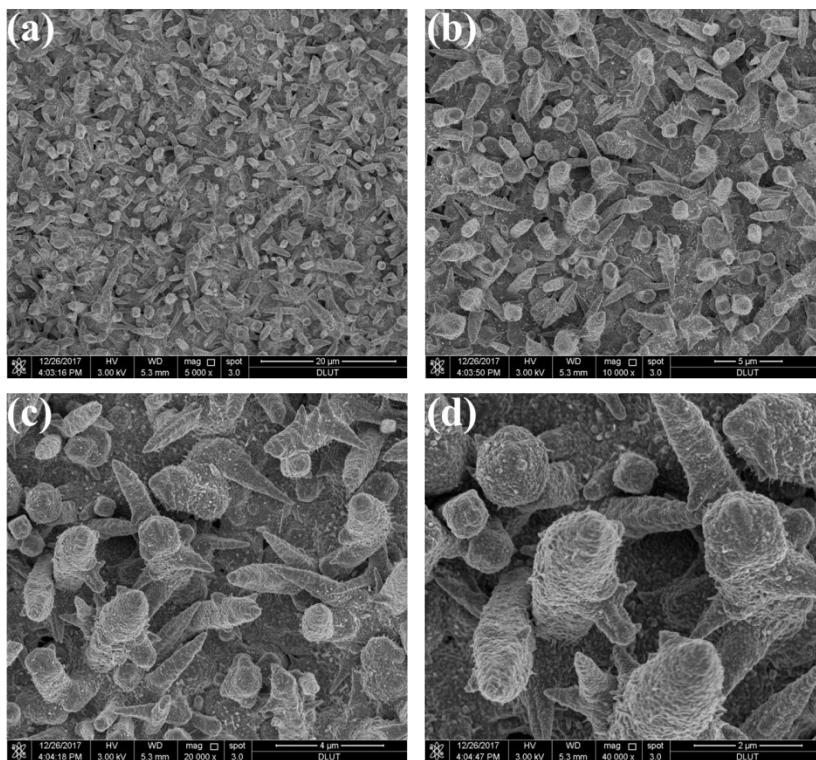


Figure S5. The SEM images of the CuO/TF electrode.

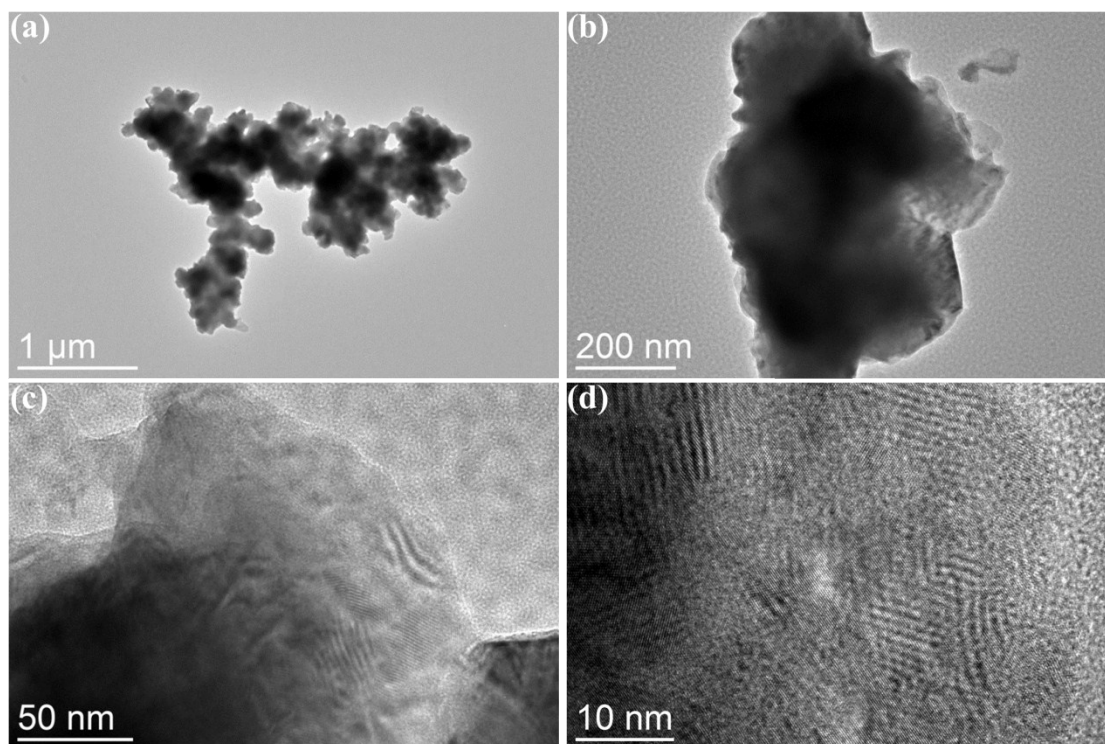


Figure S6. The TEM images of the $\text{Cu}_2\text{Se-Cu}_2\text{O}$ sample scraped from the $\text{Cu}_2\text{Se-Cu}_2\text{O}$ /TF electrode.

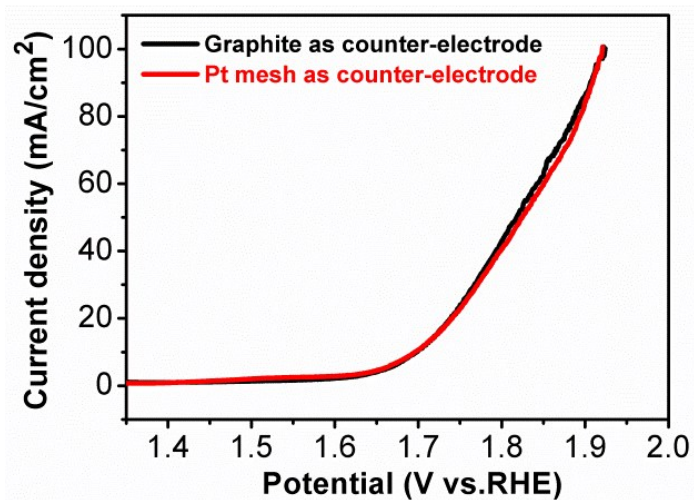


Figure S7. Blank line: electrocatalytic activities of the $\text{Cu}_2\text{Se-Cu}_2\text{O/TF}$ electrode (a graphite rod electrode was used during preparation of the electrode) using the graphite counter electrode in 0.2 M carbonate buffer solution buffer (pH = 11.0). Red line: electrocatalytic activities of the $\text{Cu}_2\text{Se-Cu}_2\text{O/TF}$ electrode (Pt mesh electrode was used during preparation of the electrode) using the Pt counter electrode in 0.2 M carbonate buffer solution buffer (pH = 11.0).

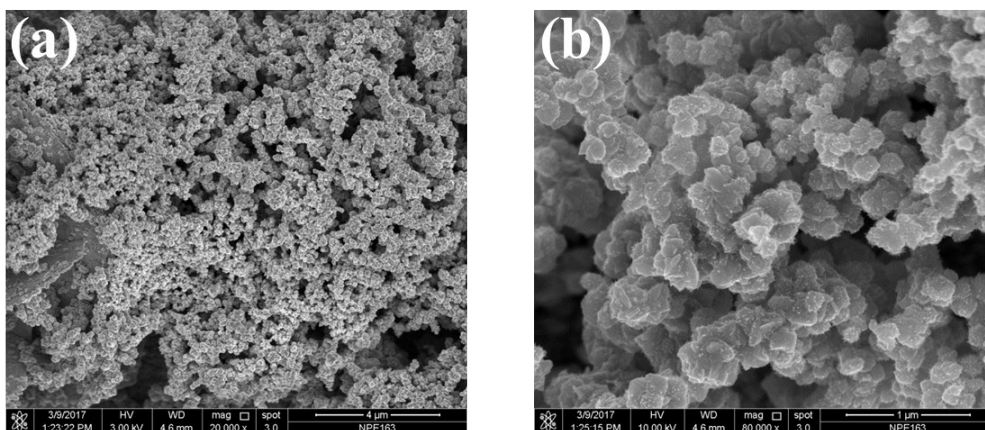


Figure S8. The SEM images of $\text{Cu}_2\text{Se-Cu}_2\text{O/Ti}$ foil after OER.

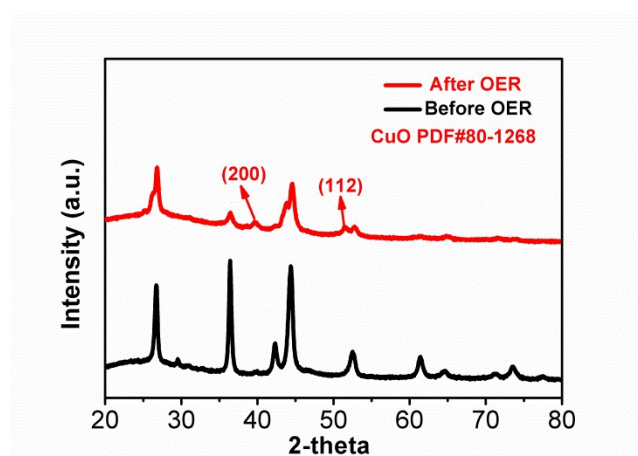


Figure S9. The powder XRD spectra of the $\text{Cu}_2\text{Se-Cu}_2\text{O}$ materials before and after OER.

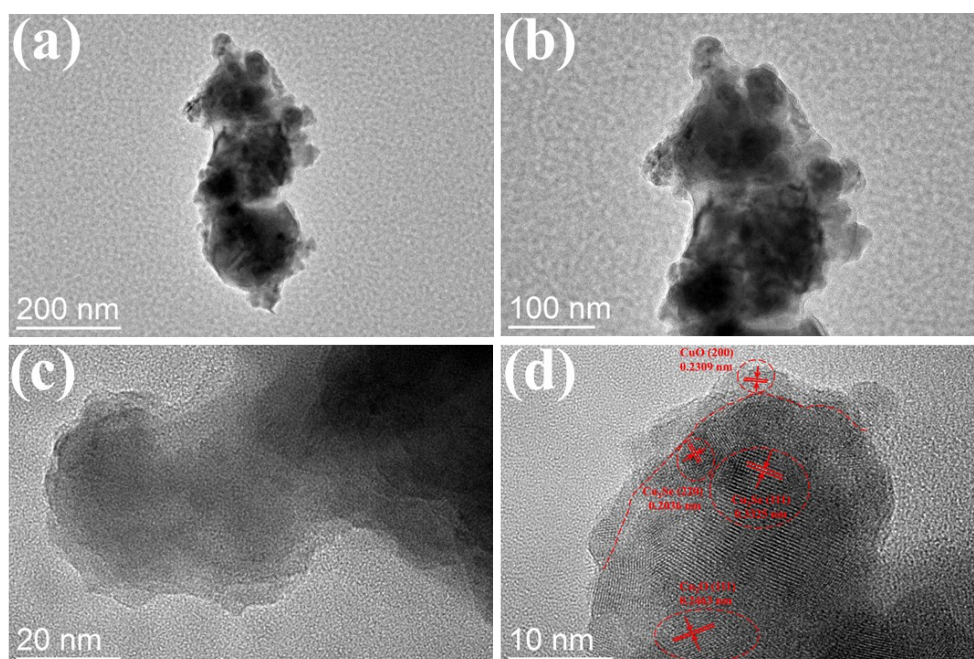


Figure S10. The TEM images of the $\text{Cu}_2\text{Se-Cu}_2\text{O}$ sample scraped from the TF substrate after the OER.

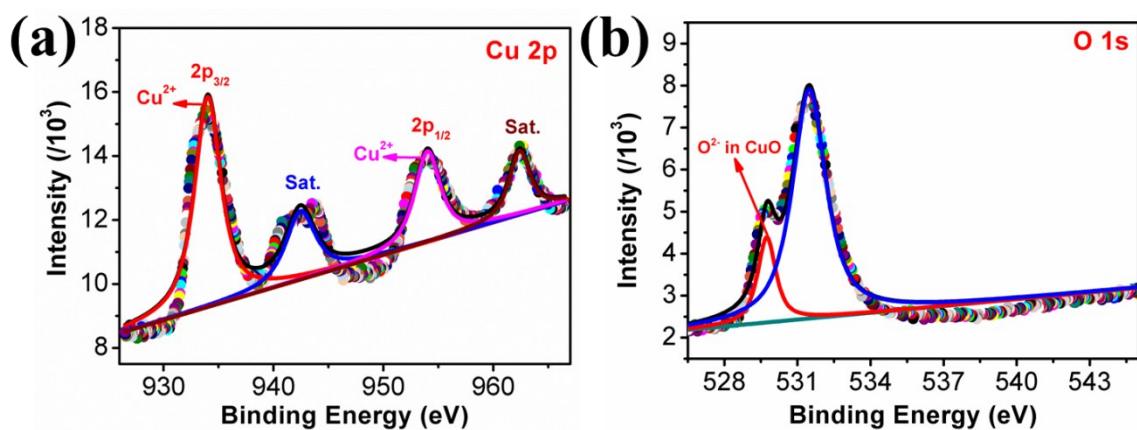


Figure S11. The high-resolution XPS spectra of Cu 2p (a) and O 1s (b) of the $\text{Cu}_2\text{Se-Cu}_2\text{O/TF}$ electrode after OER.

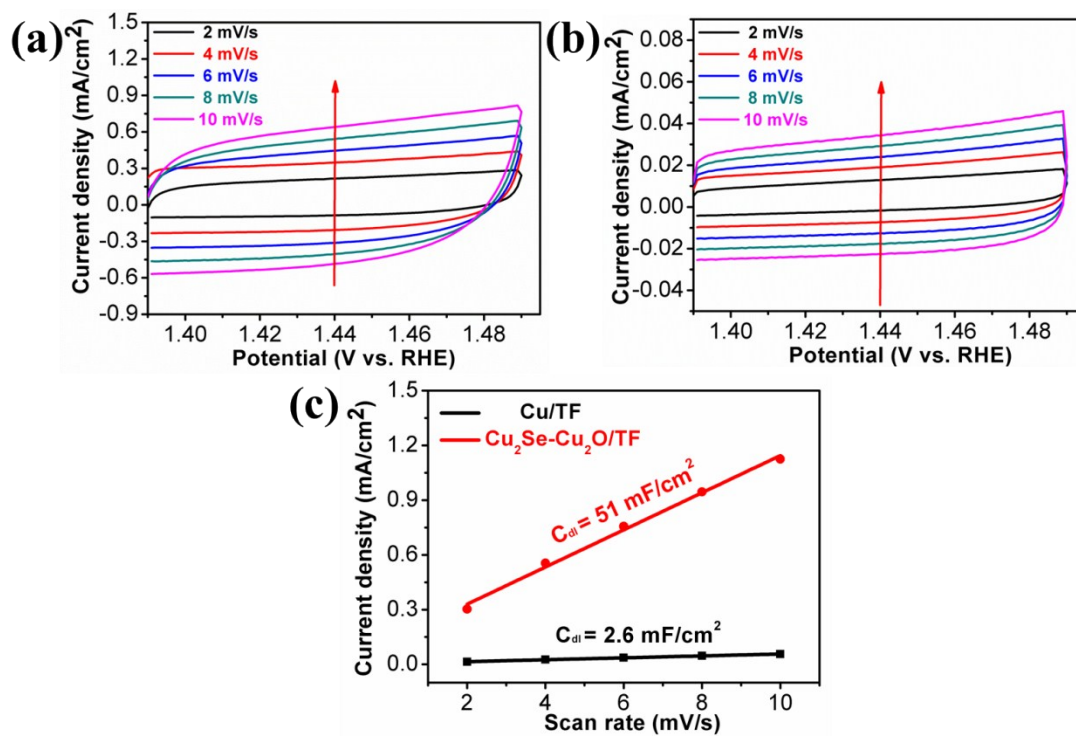


Figure S12. CV curves of the electrodes Cu/TF (a) and $\text{Cu}_2\text{Se/Cu}_2\text{O/TF}$ (b) in 0.2 M carbonate buffer solution buffer ($\text{pH} = 11.0$) under different scan rates; (c) Plots of i_c vs. scan rates v .

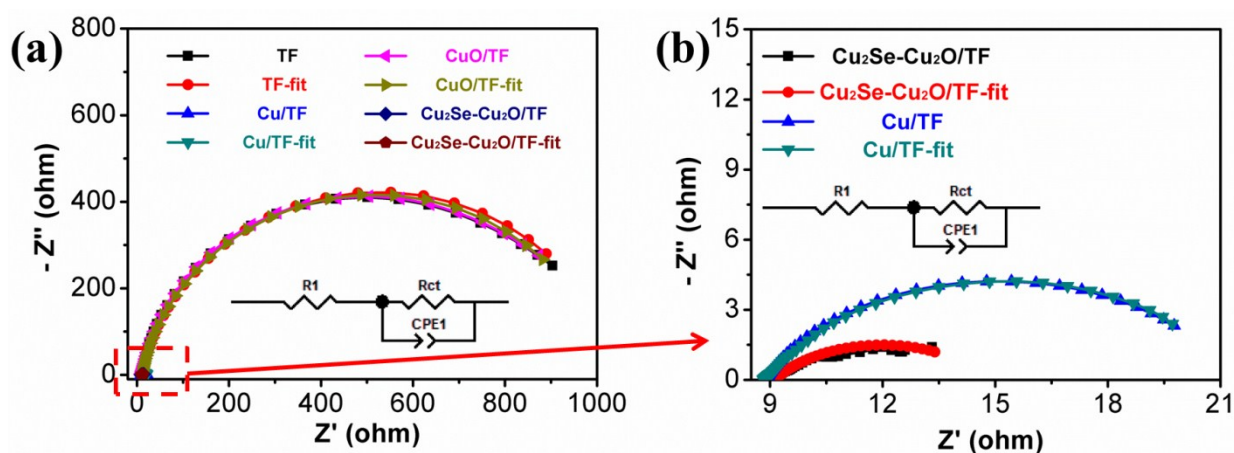


Figure S13. EIS spectra of the TF, Cu/T, CuO/TF and Cu₂Se-Cu₂O/TF electrode.

Table S1. Comparison of copper-based heterogeneous electrocatalysts for OER

Catalyst	Substrate	Electrolyte	pH	η (mV) @ the corresponding i (mA/cm ²)	Ref.
Cu-bifunctional	FTO	0.1 M Bi buffer	9.2	749 mV @ 1.0 mA/cm ²	1
CuO nanowire	FTO	0.1 M Bi buffer	9.2	550 mV @ 1.0 mA/cm ²	2
CuO	Cu foil	1 M Na ₂ CO ₃	10.8	580 mV @ 10.0 mA/cm ²	3
CuO from Cu-TEOA	ITO	0.1 M Ac buffer	12.4	780 mV @ 1.0 mA/cm ²	4
Cu₂S Nanoplate	GC	0.25 M Pi buffer	13.0	428 mV @ 10.0 mA/cm ²	5
CuO from Cu-en	ITO	0.2 M Pi buffer	12.0	550 mV @ 1.0 mA/cm ²	6
Leaf-type CuO	Cu foil	0.2 M Ci buffer	11.0	450 mV @ 10.0 mA/cm ²	7
CuO from Cu-Tris	ITO	0.2 M, Pi buffer	12.0	390 mV @ 1.0 mA/cm ²	8
Cu(OH)₂	FTO	0.1 M Bi buffer	9.2	655 mV @ 1.0 mA/cm ²	9
Cu₂Se-Cu₂O	Ti foil	0.2 M Ci buffer	11.0	465 mV @ 10.0 mA/cm ²	This work

Note: The η is overpotential, the i is the electrocatalytic current density, the FTO is fluorine-doped tin oxide glass, the ITO is indium tin oxide glass, the GC is glass carbon electrode. Bi is borate buffer solution, Pi is phosphate buffer solution, Ac is acetate buffer solution and Ci is carbonate buffer solution.

References

1. X. Liu, H. Zheng, Z. Sun, A. Han, P. Du, *ACS Catal.*, 2015, **5**, 1530.
2. X. Liu, S. Cui, Z. Sun, P. Du, *Electrochim. Acta*, 2015, **160**, 202.
3. J. Du, Z. Chen, S. Ye, B.J. Wiley, T.J. Meyer, *Angew. Chem. Int. Ed.*, 2015, **54**, 2073.
4. T. Li, S. Cao, C. Yang, Y. Chen, X. Lv, W. Fu, *Inorg. Chem.*, 2015, **54**, 3061.
5. L. An, P. Zhou, J. Yin, H. Liu, F. Chen, H. Liu, Y. Du, P. Xi, *Inorg. Chem.*, 2015, **54**, 3281.
6. C. Lu, J. Du, X. Su, M. Zhang, X. Xu, T.J. Meyer, Z. Chen, *ACS Catal.*, 2016, **6**, 77.
7. K.S. Joya, H.J.M. de Groot, *ACS Catal.*, 2016, **6**, 1768.
8. H. Chen, Y. Gao, Z. Lu, L. Ye, L. Sun, *Electrochim. Acta*, 2017, **230**, 501.
9. S. Cui, X. Liu, Z. Sun, P. Du, *ACS Sustainable Chem. Eng.*, 2016, **4**, 2593.